PHYSICS

Pristine quantum criticality in a Kondo semimetal

Wesley T. Fuhrman[1†‡], Andrey Sidorenko[2†], Jonathan Hänel[2], Hannes Winkler[2], Andrey Prokofiev[2], Jose A. Rodriguez-Rivera[3,4], Yiming Qiu[4], Peter Blaha[5], Qimiao Si[6], Collin L. Broholm[1,4,7], Silke Paschen[2,6]*

The observation of quantum criticality in diverse classes of strongly correlated electron systems has been instrumental in establishing ordering principles, discovering new phases, and identifying the relevant degrees of freedom and interactions. At focus so far have been insulators and metals. Semimetals, which are of great current interest as candidate phases with nontrivial topology, are much less explored in experiments. Here, we study the Kondo semimetal $CeRu_4Sn_6$ by magnetic susceptibility, specific heat, and inelastic neutron scattering experiments. The power-law divergence of the magnetic Grünesien ratio reveals that, unexpectedly, this compound is quantum critical without tuning. The dynamical energy over temperature scaling in the neutron response throughout the Brillouin zone and the temperature dependence of the static uniform susceptibility, indicate that temperature is the only energy scale in the criticality. Such behavior, which has been associated with Kondo destruction quantum criticality in metallic systems, could be generic in the semimetal setting.

INTRODUCTION

Quantum criticality is observed in many strongly correlated materials classes, with quantum spin systems (1), high-T_c cuprate (2) and iron pnictide (3) superconductors, and heavy fermion metals (4–6) being prominent examples. Among them, the quantum critical insulators are the best understood. For instance, in the insulating quantum magnet $LiHoF_4$ (7), the experimentally detected quantum criticality is well described in terms of the Landau framework, i.e., by the critical fluctuations of the magnetic order parameter (8, 9). In quantum critical metals, by contrast, the underlying physics is much richer. In some systems, the Landau description works well (10, 11), but in others, it appears to fail (5, 6, 12). Theoretically, the charge carriers introduce additional nontrivial couplings to the order parameter or its underlying building blocks, which opens new possibilities for quantum criticality (13–15).

Here, we explore the case of the Kondo semimetal $CeRu_4Sn_6$. Its noncentrosymmetric crystal structure (Fig. 1A), strong spin-orbit coupling associated with the three large atomic-number elements, and the fact that the anisotropy in its electronic dispersion (16) cannot be attributed to a nodal ground-state wave function of the $Ce^{3+}4f^1$ electron (17) have led to speculations (17) that the material may be topologically nontrivial. Density functional theory (DFT) calculation within the local density approximation (LDA) and the Gutzwiller scheme predict the material to host Weyl nodes (18). If the nodal excitations persist in a full treatment of the Kondo effect, then $CeRu_4Sn_6$ will be a Weyl-Kondo semimetal (19–21). Our comprehensive investigation of the magnetization, Grüneisen parameter, and inelastic neutron scattering as functions of temperature and magnetic field reveals that this material is quantum critical without tuning, behavior that is only rarely observed (22). This raises the exciting question of whether a Weyl-Kondo semimetal phase may indeed be located nearby, nucleating out of the quantum critical fluctuations.

RESULTS AND DISCUSSION

The semimetallic character of $CeRu_4Sn_6$ (see the Supplementary Materials for information on crystal growth and characterization) is evidenced by the weak temperature dependence of the electrical resistivity below about 30 K and the small low-temperature charge carrier concentration (Fig. 1B). We have also measured the temperature dependence of the specific heat C_p (Fig. 1C) and the magnetization M, the latter with different magnetic fields H applied along the two main crystallographic directions (perpendicular and parallel to c; Fig. 1, D and E, respectively). The high-temperature anisotropy was recently shown to be due to single-ion crystal-field effects on the $Ce^{3+}4f^1$ electrons (23). Deviations from this behavior below room temperature indicate a partial gapping of the electronic density of states and/or the onset of Kondo screening (23). Below 10 K, a strong field dependence is observed. The temperature dependence of the magnetic susceptibility $\chi = M/H|_{10\,mT}$ is not of simple Curie-Weiss type [$\chi = C/(T - \Theta)$] but, instead, is well described by

$$\frac{1}{\chi(T)} = \frac{1}{\chi(T=0)} + \frac{(a\,T)^\alpha}{c} \qquad (1)$$

with $\alpha = 0.50 \pm 0.01$ and $\alpha = 0.78 \pm 0.03$ for magnetic fields applied perpendicular and parallel to c, respectively (Fig. 1, D and E, insets). This is inconsistent with quantum criticality involving a Lorentzian fluctuation spectrum, where $\alpha = 1$ (Curie-Weiss law) is expected. The application of larger magnetic fields gradually restores Fermi liquid behavior, i.e., a temperature-independent low-temperature magnetization (Fig. 1, D and E, main panels).

The magnetic Grüneisen ratio $\Gamma_{mag} = -(\partial M/\partial T)/C_p$ is expected to diverge at any quantum critical point (24), as observed in a number of quantum critical heavy fermion metals (25, 26). For $CeRu_4Sn_6$,

[1]Institute for Quantum Matter and Department of Physics and Astronomy, The Johns Hopkins University, Baltimore, MD 21218, USA. [2]Institute of Solid State Physics, Vienna University of Technology, Wiedner Hauptstr. 8-10, 1040 Vienna, Austria. [3]Department of Materials Sciences, University of Maryland, College Park, MD 20742, USA. [4]NIST Center for Neutron Research, National Institute of Standards and Technology, Gaithersburg, MD 20899, USA. [5]Institute of Materials Chemistry, Vienna University of Technology, 1040 Vienna, Austria. [6]Department of Physics and Astronomy, Rice Center for Quantum Materials, Rice University, Houston, TX 77005, USA. [7]Department of Materials Science and Engineering, The Johns Hopkins University, Baltimore, MD 21218, USA.
*Corresponding author. Email: paschen@ifp.tuwien.ac.at
†These authors contributed equally to this work.
‡Present address: The Johns Hopkins Applied Physics Laboratory , Laurel, MD 20723, USA.
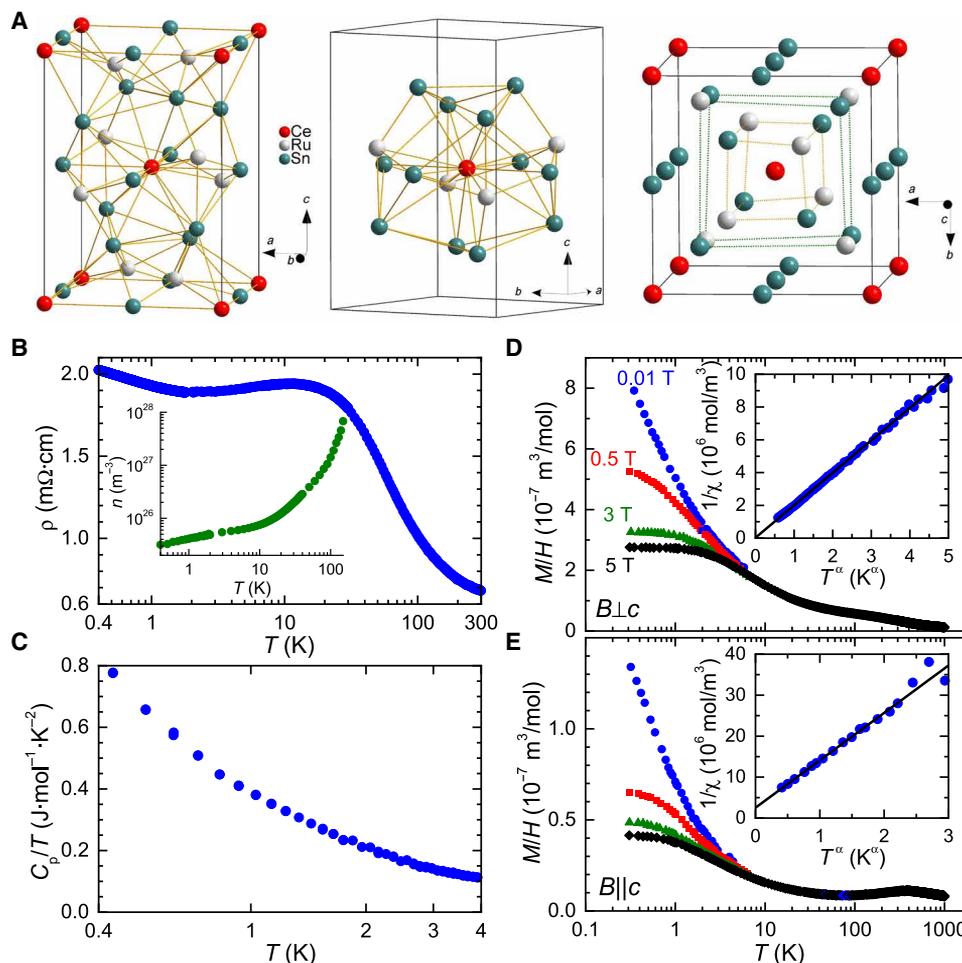
Fig. 1. Characterization of CeRu₄Sn₆. (**A**) Unit cell with view along tetragonal direction $a = b$ (left), polyhedron around central Ce atom (center), and unit cell with view along c of the noncentrosymmetric tetragonal $\bar{I}42m$ crystal structure of CeRu₄Sn₆, with $a = 6.8810$ Å and $c = 9.7520$ Å (*37*, *38*). (**B**) Electrical resistivity (main panel) and charge carrier concentration determined from Hall effect measurements in a simple one-band model (inset) versus temperature, with current within the tetragonal plane, evidencing the semimetallic character of CeRu₄Sn₆. (**C**) Low-temperature specific heat over temperature ratio, plotted on semilogarithmic scales, evidencing a stronger than logarithmic divergence. (**D**) Magnetization over magnetic field, measured in different magnetic fields ($B = \mu_0 H$) applied perpendicular to the tetragonal c axis, as function of temperature. The inset shows the inverse susceptibility, defined as $1/\chi = H/M|_{10\,mT}$, plotted versus T^α, with $\alpha = 0.50 \pm 0.01$ as determined from a least-square fit with $1/\chi = 1/\chi_0 + c \cdot T^\alpha$ to the data below 10 K. (**E**) Same as (D) for magnetic fields applied along c, with $\alpha = 0.78 \pm 0.03$. The fit was done below 3 K, where the noise in the data is small [c is the hard direction, along which χ is much smaller; note the different scales of (D) and (E)].

from the low-field (10 mT) magnetization and specific heat data presented above, we find $\Gamma_{\text{mag}} \sim T^{-\epsilon}$ between about 0.4 K and 4 K, with $\epsilon = 1.43 \pm 0.07$ and 1.62 ± 0.11 for fields perpendicular and parallel to the c axis, respectively (Fig. 2, A and B), providing strong evidence for quantum criticality without tuning in CeRu₄Sn₆.

The field and temperature scaling of the magnetization data underpins this assignment. In Fig. 2 (C and D), we plot $-\partial(M/H)/\partial T \cdot H^\beta$ versus T/H^γ over more than two orders of magnitude in T/H^γ, for fields between 10 mT and 0.5 T both perpendicular and parallel to c. We find a good data collapse with the exponents β being equal to α extracted from Fig. 1 (D and E) (insets) and $\gamma = 0.35 \pm 0.02$ and 0.43 ± 0.02 for fields perpendicular and parallel to c, respectively. The fitted exponents are internally consistent, as they satisfy a scaling relationship (see the Supplementary Materials). This kind of critical scaling, with a fractional exponent $\alpha < 1$ (*13*), indicates that the system is at, or very close to, a beyond-Landau quantum critical

point and that magnetic field acts as a tuning parameter, with criticality at $H = 0$.

This is corroborated by our neutron scattering investigation presented next. The inelastic neutron scattering intensity is dominated by features broad in momentum space, with no apparent energy scale, setting the lower bound for a gap in the spin excitations to less than 0.1 meV. In Fig. 3 (A to C), we show the intensity distribution at 1.5 K, integrated from 0.2 meV to 1.2 meV, in the (H0L), (HK0), and (HHL) planes, respectively. The energy profile along two high-symmetry directions, (00L) and (H00), integrated over ±0.2 reciprocal lattice units (r.l.u.) perpendicular to these directions, is presented in Fig. 3 (D and E). The strong peaks at H + K + L = even are tails of nonmagnetic elastic Bragg scattering. There is no apparent change in the momentum dependence with energy transfer, meaning that the **q** and ω dependence of the scattering cross section factorizes and there is no dispersion. This is clearly at odds with any description of
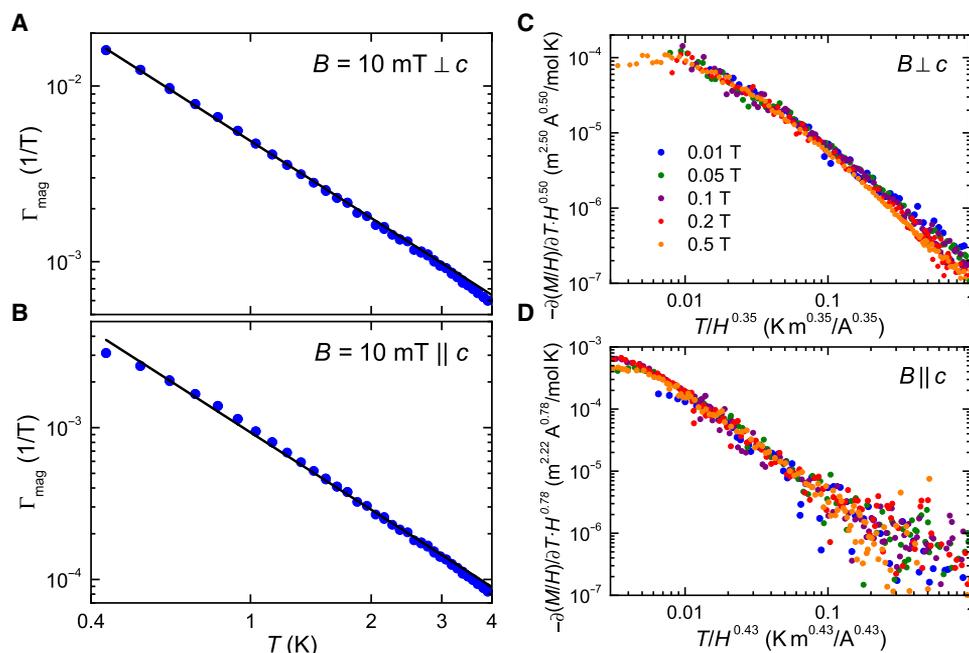
**Fig. 2. Signatures of quantum criticality in thermodynamic properties of CeRu$_4$Sn$_6$.** (**A**) Magnetic Grüneisen ratio Γ_{mag} versus temperature at $B = \mu_0 H = 10$ mT, applied perpendicular to the c axis, with a power law fit to the data (exponent 1.43 ± 0.07). (**B**) Same as (A) for magnetic fields applied along c, with exponent 1.62 ± 0.11. (**C**) Scaled negative temperature derivative of the magnetization over field ratio, $-\partial(M/H)/\partial T \cdot H^\beta$ versus scaled temperature, T/H^γ, for fields perpendicular to c, with exponents β and γ that collapse the data. (**D**) Same as (C) for magnetic fields applied along c.
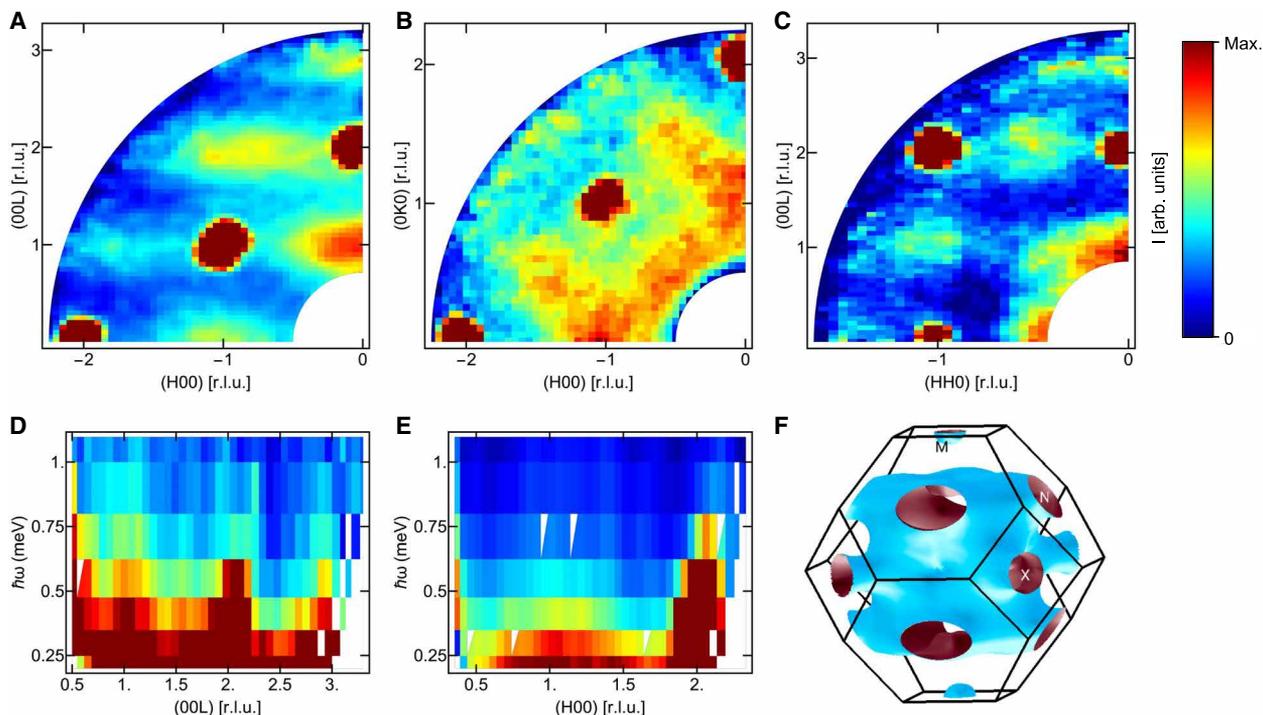
Fig. 3. Quasielastic neutron scattering from CeRu$_4$Sn$_6$. (**A** to **C**) Energy-integrated neutron scattering intensity at 1.5 K in the (H0L), (HK0), and (HHL) planes, respectively. Saturated intensity at H + K + L = even is residual Bragg intensity. Along $\left(\frac{1}{2} + H, \frac{1}{2} - H, 0\right)$ and equivalent directions in (B) and, to a lesser extent, along (H00) centered at H + 0 + L = odd in (A), the scattering intensity is almost **q**-independent. (**D** and **E**) Neutron scattering cross section versus energy and momentum transfer along (00L) and (H00), respectively. The **q** and ω dependence of the scattering cross section factorizes so that there is no dispersion and the signal continues below the resolution limit of the instrument. (**F**) "f-core" Fermi surface derived from LDA-DFT calculations.

the criticality in terms of the fluctuations of an incipient symmetry-breaking order parameter, where the scattering intensity should be increasingly peaked at the critical wave vector. The broadness of the features is especially pronounced along $\left(\frac{1}{2} + H, \frac{1}{2} - H, 0\right)$ (Fig. 3B) and, to a lesser extent, along the (H00) direction for peak intensities at H + 0 + L = odd (Fig. 3A) and symmetry-related directions where the scattering intensity simply follows the magnetic form factor of the $Ce^{3+} 4f^1$ electrons. Scattering that is momentum independent along lines in the Brillouin zone is a sign of local (or Kondo destruction) quantum criticality (13) and has also been observed in quantum critical $CeCu_{5.9}Au_{0.1}$ (12). The wave vector dependence of the scattering intensity away from these high-intensity lines is discussed below.

First, however, we investigate whether quantum critical scaling, as evidenced by the static uniform magnetic susceptibility $\chi = (\partial M / \partial H)_{H \to 0} = \chi'(\mathbf{q} = 0, \omega = 0, T)$ (Fig. 1, D and E, insets), is also found in the dynamical spin susceptibility $\chi(\mathbf{q}, \omega, T)$. This would give rise to the form

$$\chi(\mathbf{q}, \omega, T) = \frac{c}{f(\mathbf{q}) + (-i\hbar\omega + a\,T)^{\alpha}} \qquad (2)$$

where $f(\mathbf{q})$ is an offset and $\alpha = 1$ is expected for a Lorentzian fluctuation spectrum as prescribed by the Landau order parameter description (8, 9), and a fractional exponent $\alpha < 1$ points to its failure. The dynamic structure factor $\mathcal{S}(\mathbf{q}, \omega, T)$ measured by inelastic neutron scattering is related to the imaginary part χ'' of $\chi(\mathbf{q}, \omega, T)$ by $\chi'' = \mathcal{S} \cdot [1 - \exp(-\hbar\omega/k_B T)]$, where the second factor manifests the fluctuation-dissipation relation. Near the peak wave vector, where the singular susceptibility corresponds to a vanishing $f(\mathbf{q})$, it takes the form

$$\chi''(\omega, T) = \frac{1}{T^{\alpha}} \cdot g(\hbar\omega/k_B T) \qquad (3)$$

where g is a function that depends only on the ratio of $\hbar\omega$ and $k_B T$. We have determined $\mathcal{S}(\omega, T)$ by integrating the neutron scattering intensity for momentum transfers $\mathbf{q}$ about the (100) wave vector (where the quasielastic intensity is maximal; see Fig. 3, A and B), and plot it for temperatures between 0.1 K and 10 K, and energy transfers between 0.1 meV and 1.3 meV as $\mathcal{S} \cdot T^{\alpha}$ versus $\hbar\omega/k_B T$ in Fig. 4A. The best data collapse is found for $\alpha = 0.6 \pm 0.1$ (inset of Fig. 4A). This is consistent with the α values determined from the static uniform magnetic susceptibility ($\alpha = 0.50 \pm 0.01$ for $H \perp c$ and $\alpha = 0.78 \pm 0.03$ for $H \parallel c$), in particular, in view of the fact that the neutron scattering intensity is a directional average, taken around the (100) wave vector, where spin fluctuations polarized along and perpendicular to c contribute in equal measures. Thus, also the inelastic neutron scattering data evidence quantum criticality beyond the long-wavelength fluctuations of an order parameter (8, 9), such as expected in the theory of Kondo destruction quantum criticality (13).

Last, we turn to the spatial profile of the critical fluctuations. To do so, we have fitted the experimental scattering intensity, corrected for the Ce form factor, in terms of Eq. 2. The resulting $f(\mathbf{q})$ in the (H0L) and (HK0) planes are shown in Fig. 4 (B and C, respectively). For the rather featureless $\left(\frac{1}{2} + H, \frac{1}{2} - H, 0\right)$ "ridge," the singular dynamical spin susceptibility discussed earlier corresponds to a vanishingly small $f(\mathbf{q})$ (see Fig. 4C). Likewise, in the (H0L) plane, it is seen that $f(\mathbf{q})$ is vanishingly small for H + 0 + L = odd, where the dynamical spin susceptibility is also peaked. Along directions that move away from these ridges, the decreasing dynamical spin susceptibility corresponds to an increasing $f(\mathbf{q})$. We can understand
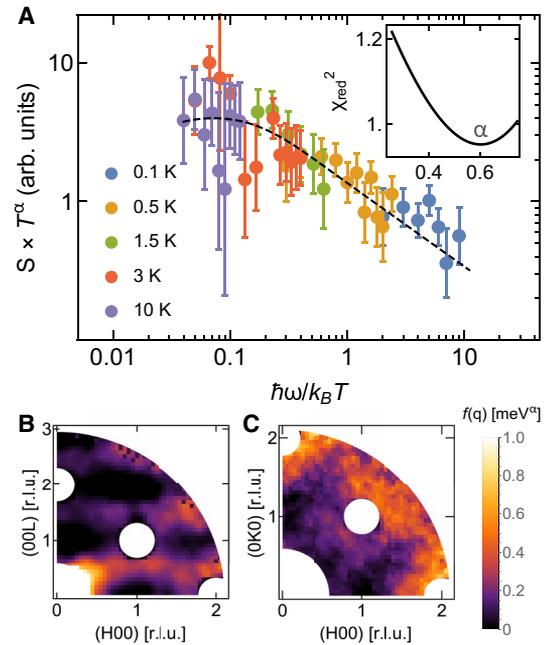

Fig. 4. Dynamical scaling of CeRu$_4$Sn$_6$. (**A**) Scaled neutron scattering intensity, $\mathcal{S} \cdot T^{\alpha}$, from data collected at (100) and integrated over 0.2 r.l.u. along (H00) and (00L), versus scaled energy transfer, $\hbar\omega/k_B T$. The dashed line is the best fit of the function $\mathcal{S} \cdot T^{\alpha} = g(\hbar\omega/k_B T)/[1 - \exp(-\hbar\omega/k_B T)]$ to the data, as obtained from Eq. 2 for $f(\mathbf{q}) = 0$ [which holds well as seen from (B) and (C)]. The inset shows the reduced deviation between data and fit, χ_{red}^2, determined as the variance (squared sum of fit residuals divided by the degrees of freedom $n - p$, where n is the number of data points and p the number of fit parameters; the nonuniversal parameters a and c are left open), which is minimal for $\alpha = 0.6$. (**B** and **C**) Offset $f(\mathbf{q})$ from Eq. 2 in the (H0L) and (HK0) plane, respectively, obtained through a global fit of Eq. 2 to the $\mathbf{q} - E-$ dependent data in Fig. 3 with a single consistent value of α. The white areas correspond to blinded out data near the nuclear Bragg peaks, which are situated at H + K + L = even. Along $\left(\frac{1}{2} + H, \frac{1}{2} - H, 0\right)$ in (C) and about (H01) in (B), $f(\mathbf{q})$ is minimal, indicating maximally antiferromagnetic interactions (see the main text).

these features of $f(\mathbf{q})$ in terms of the wave vector dependence of the Ruderman-Kittel-Kasuya-Yosida (RKKY) interaction

$$J(\mathbf{q}) = J_K^2 L(\mathbf{q}, \omega = 0) = J_K^2 \sum_{\mathbf{k}} \frac{f(\varepsilon_{\mathbf{k}}) - f(\varepsilon_{\mathbf{k+q}})}{\varepsilon_{\mathbf{k+q}} - \varepsilon_{\mathbf{k}}}. \qquad (4)$$

Here, J_K is the Kondo coupling strength and $L(\mathbf{q}, \omega)$ the Lindhard function of the (uncorrelated) conduction electrons, which we have determined through LDA-DFT calculations, with one $4f$ electron per Ce^{3+} ion placed in the ionic core. This "f-core" band structure, resembling that of $LaRu_4Sn_6$, characterizes the electronic structure of the spd conduction electrons that mediate the RKKY interaction between the $4f$ moments. The associated Fermi surface is shown in Fig. 3F, from which we can identify nesting wave vectors that correspond to the $\left(\frac{1}{2} + H, \frac{1}{2} - H, 0\right)$ and H + 0 + L = odd ridges. These can be seen as the broad planes perpendicular to the (00L) direction (Γ to M) and between X points extending along (00L). At these wave vectors, collectively denoted as $\mathbf{Q}$, the RKKY interaction is maximally antiferromagnetic. The Weiss temperature scale

$$\Theta(\mathbf{q}) = J(\mathbf{q}) - J(\mathbf{Q}) \qquad (5)$$

describes the offset $f(\mathbf{q})$, when the latter is raised to the power $1/\alpha$. In other words, the neutron scattering intensity is maximal where the Weiss temperature $\Theta(\mathbf{q})$ has a minimum, implying that the RKKY interaction defines the $\mathbf{q}$ space structure. Accordingly, the system may be near antiferromagnetic order mediated by the RKKY interaction, with an ordering wave vector at H + K + L = odd.

Beyond-Landau quantum criticality, as indicated by a fractional exponent $\alpha < 1$, has been documented in a handful of other heavy fermion compounds (12, 22, 27–29). Except for the case of the heavy fermion metal $CeCu_{5.9}Au_{0.1}$, a determination of α from inelastic neutron scattering—as provided here—has, however, remained elusive. Our discovery of beyond-Landau quantum criticality, in both the inelastic neutron response and the static uniform magnetic susceptibility, in a genuinely quantum critical semimetal implicates the generality of the phenomenon. Because this constitutes the first observation of this phenomenon in a semimetal, it will be important to explore whether beyond-Landau quantum criticality is inherent to systems with reduced charge carrier concentration. Promising materials to explore in this context are the low-carrier density Kondo systems $CeRhBi$ (30), $CeNi_{2-\delta}As_2$ (31), and $Yb_3Ir_4Ge_{13}$ (32), as well as the pyrochlore iridate $Pr_2Ir_2O_7$ (33, 34), which all show thermodynamic signatures of quantum criticality.

In heavy fermion systems, quantum criticality is generally observed at the $T = 0$ collapse of (antiferromagnetically) ordered phases. $CeRu_4Sn_6$, however, is quantum critical without tuning pressure, stoichiometry, or applied fields to a phase boundary. A natural question then arises: Is an antiferromagnetic phase nearby, as suggested by the minima of the Weiss temperature near possible antiferromagnetic ordering wave vectors, and can it be reached by tuning, for instance with pressure? And even more excitingly, do the quantum critical fluctuations give rise to emergent phases, maybe unconventional superconductivity in analogy to β-$YbAlB_4$ (35) or, in view of all the necessary conditions being fulfilled, even a Weyl-Kondo semimetal phase akin to that recently discovered in $Ce_3Bi_4Pd_3$ (19–21)? This will require further experiments at lower temperatures and as function of tuning parameters, which we hope this work will stimulate.

MATERIALS AND METHODS

For our study, single crystals of $CeRu_4Sn_6$ were grown from self-flux, using the floating zone melting technique with optical heating as reported previously (36) (see the Supplementary Materials for further details). The magnetic properties between 2 K and 300 K were measured in a SQUID magnetometer from Cryogenic Ltd., and the data between 0.3 K and 2 K used a ^{3}He insert. High-temperature magnetization measurements up to 1000 K were performed with a vibrating sample magnetometer in a Physical Properties Measurement System (PPMS) from Quantum Design. The ^{3}He PPMS option was used for specific heat measurements in the temperature range from 0.3 K to 20 K.

Neutron scattering was performed with the Multi Axis Crystal Spectrometer (MACS) at the National Institute of Standards and Technology Center for Neutron Research. For the momentum-space mapping, we co-aligned 3 g of single crystals and used incident energies from 3.7 meV to 5 meV and a fixed final energy of 3.7 meV, allowing for the use of Be and BeO filters before and after the sample, respectively, and providing an effective resolution better than 0.05 Å^{-1} and 0.15 meV. For the ω/T scaling measurements, 2 g of single crystals were accommodated within the restrictions of a dilution refrigerator.

We used a fixed final energy of 2.5 meV and incident energies up to 3.7 meV. A magnetic field of 10 mT was applied along (0K0) to avoid superconductivity in the aluminum sample mount and maintain good thermal contact.

SUPPLEMENTARY MATERIALS

Supplementary material for this article is available at http://advances.sciencemag.org/cgi/content/full/7/21/eabf9134/DC1

REFERENCES AND NOTES

1. R. Coldea, D. A. Tennant, E. M. Wheeler, E. Wawrzynska, D. Prabhakaran, M. Telling, K. Habicht, P. Smeibidl, K. Kiefer, Quantum criticality in an Ising chain: Experimental evidence for emergent E_8 symmetry. *Science* **327**, 177–180 (2010).
2. S. Sachdev, Where is the quantum critical point in the cuprate superconductors? *Phys. Status Solidi B* **247**, 537–543 (2010).
3. J. Dai, Q. Si, J. X. Zhu, E. Abrahams, Iron pnictides as a new setting for quantum criticality. *Proc. Natl. Acad. Sci. U.S.A.* **106**, 4118–4121 (2009).
4. H. v. Löhneysen, A. Rosch, M. Vojta, P. Wölfle, Fermi-liquid instabilities at magnetic quantum phase transitions. *Rev. Mod. Phys.* **79**, 1015–1075 (2007).
5. S. Kirchner, S. Paschen, Q. Chen, S. Wirth, D. Feng, J. D. Thompson, Q. Si, Colloquium: Heavy-electron quantum criticality and single-particle spectroscopy. *Rev. Mod. Phys.* **92**, 011002 (2020).
6. S. Paschen, Q. Si, Quantum phases driven by strong correlations. *Nat. Rev. Phys.* **3**, 9–26 (2021).
7. D. Bitko, T. F. Rosenbaum, G. Aeppli, Quantum critical behavior for a model magnet. *Phys. Rev. Lett.* **77**, 940–943 (1996).
8. J. A. Hertz, Quantum critical phenomena. *Phys. Rev. B* **14**, 1165–1184 (1976).
9. A. J. Millis, Effect of a nonzero temperature on quantum critical points in itinerant fermion systems. *Phys. Rev. B* **48**, 7183–7196 (1993).
10. R. Küchler, N. Oeschler, P. Gegenwart, T. Cichorek, K. Neumaier, O. Tegus, C. Geibel, J. A. Mydosh, F. Steglich, L. Zhu, Q. Si, Divergence of the Grüneisen ratio at quantum critical points in heavy fermion metals. *Phys. Rev. Lett.* **91**, 066405 (2003).
11. R. Jaramillo, Y. Feng, J. Wang, T. F. Rosenbaum, Signatures of quantum criticality in pure Cr at high pressure. *Proc. Natl. Acad. Sci. U.S.A.* **107**, 13631–13635 (2010).
12. A. Schröder, G. Aeppli, R. Coldea, M. Adams, O. Stockert, H. Löhneysen, E. Bucher, R. Ramazashvili, P. Coleman, Onset of antiferromagnetism in heavy-fermion metals. *Nature* **407**, 351–355 (2000).
13. Q. Si, S. Rabello, K. Ingersent, J. L. Smith, Locally critical quantum phase transitions in strongly correlated metals. *Nature* **413**, 804–808 (2001).
14. S.-S. Lee, Low-energy effective theory of Fermi surface coupled with U(1) gauge field in 2+1 dimensions. *Phys. Rev. B* **80**, 165102 (2009).
15. D. F. Mross, J. McGreevy, H. Liu, T. Senthil, Controlled expansion for certain non-Fermi-liquid metals. *Phys. Rev. B* **82**, 045121 (2010).
16. V. Guritanu, P. Wissgott, T. Weig, H. Winkler, J. Sichelschmidt, M. Scheffler, A. Prokofiev, S. Kimura, T. Iizuka, A. M. Strydom, M. Dressel, F. Steglich, K. Held, S. Paschen, Anisotropic optical conductivity of the putative Kondo insulator $CeRu_4Sn_6$. *Phys. Rev. B* **87**, 115129 (2013).
17. M. Sundermann, F. Strigari, T. Willers, H. Winkler, A. Prokofiev, J. M. Ablett, J.-P. Rueff, D. Schmitz, E. Weschke, M. M. Sala, A. Al-Zein, A. Tanaka, M. W. Haverkort, D. Kasinathan, L. H. Tjeng, S. Paschen, A. Severing, $CeRu_4Sn_6$: A strongly correlated material with nontrivial topology. *Sci. Rep.* **5**, 17937 (2015).
18. Y. Xu, C. Yue, H. Weng, X. Dai, Heavy Weyl fermion state in $CeRu_4Sn_6$. *Phys. Rev. X* **7**, 011027 (2017).
19. S. Dzsaber, L. Prochaska, A. Sidorenko, G. Eguchi, R. Svagera, M. Waas, A. Prokofiev, Q. Si, S. Paschen, Kondo insulator to semimetal transformation tuned by spin-orbit coupling. *Phys. Rev. Lett.* **118**, 246601 (2017).
20. H.-H. Lai, S. E. Grefe, S. Paschen, Q. Si, Weyl-Kondo semimetal in heavy-fermion systems. *Proc. Natl. Acad. Sci. U.S.A.* **115**, 93–97 (2018).
21. S. Dzsaber, X. Yan, M. Taupin, G. Eguchi, A. Prokofiev, T. Shiroka, P. Blaha, O. Rubel, S. E. Grefe, H. H. Lai, Q. Si, S. Paschen, Giant spontaneous Hall effect in a nonmagnetic Weyl-Kondo semimetal. *Proc. Natl. Acad. Sci. U.S.A.* **118**, e2013386118 (2021).
22. Y. Matsumoto, S. Nakatsuji, K. Kuga, Y. Karaki, N. Horie, Y. Shimura, T. Sakakibara, A. H. Nevidomskyy, P. Coleman, Quantum criticality without tuning in the mixed valence compound β-$YbAlB_4$. *Science* **331**, 316–319 (2011).
23. A. Amorese, K. Kummer, N. B. Brookes, O. Stockert, D. T. Adroja, A. M. Strydom, A. Sidorenko, H. Winkler, D. A. Zocco, A. Prokofiev, S. Paschen, M. W. Haverkort, L. H. Tjeng, A. Severing, Determining the local low-energy excitations in the Kondo semimetal $CeRu_4Sn_6$ using resonant inelastic x-ray scattering. *Phys. Rev. B* **98**, 081116 (2018).
24. L. Zhu, M. Garst, A. Rosch, Q. Si, Universally diverging Grüneisen parameter and the magnetocaloric effect close to quantum critical points. *Phys. Rev. Lett.* **91**, 066404 (2003).

25. Y. Tokiwa, T. Radu, C. Geibel, F. Steglich, P. Gegenwart, Divergence of the magnetic Grüneisen ratio at the field-induced quantum critical point in YbRh$_2$Si$_2$. *Phys. Rev. Lett.* **102**, 066401 (2009).

26. P. Gegenwart, Grüneisen parameter studies on heavy fermion quantum criticality. *Rep. Prog. Phys.* **79**, 114502 (2016).

27. K. Ishida, K. Okamoto, Y. Kawasaki, Y. Kitaoka, O. Trovarelli, C. Geibel, F. Steglich, YbRh$_2$Si$_2$: Spin fluctuations in the vicinity of a quantum critical point at low magnetic fields. *Phys. Rev. Lett.* **89**, 107202 (2002).

28. R. E. Baumbach, P. C. Ho, T. A. Sayles, M. B. Maple, R. Wawryk, T. Cichorek, A. Pietraszko, Non-Fermi-liquid behavior in the filled skutterudite compound CeRu$_4$As$_{12}$. *J. Phys. Condens. Matter* **20**, 075110 (2008).

29. E. Bauer, A. Slebarski, R. P. Dickey, E. J. Freeman, C. Sirvent, V. S. Zapf, N. R. Dilley, M. B. Maple, Electronic and magnetic investigation of the filled skutterudite compound CeRu$_4$Sb$_{12}$. *J. Phys. Condens. Matter* **13**, 5183 (2001).

30. T. Sasakawa, K. Shigetoh, D. Hirata, K. Umeo, T. Takabatake, Non-Fermi-liquid behavior in CeRhBi and valence-fluctuating behavior in CeIrSb. *Physica B* **359-361**, 111–114 (2005).

31. Y. Luo, F. Ronning, N. Wakeham, X. Lu, T. Park, Z.-A. Xu, J. D. Thompson, Pressure-tuned quantum criticality in the antiferromagnetic Kondo semimetal CeNi$_{2-\delta}$As$_2$. *Proc. Natl. Acad. Sci. U.S.A.* **112**, 13520–13524 (2015).

32. B. K. Rai, I. W. H. Oswald, W. Ban, C. L. Huang, V. Loganathan, A. M. Hallas, M. N. Wilson, G. M. Luke, L. Harriger, Q. Huang, Y. Li, S. Dzsaber, J. Y. Chan, N. L. Wang, S. Paschen, J. W. Lynn, A. H. Nevidomskyy, P. Dai, Q. Si, E. Morosan, Low-carrier density and fragile magnetism in a Kondo lattice system. *Phys. Rev. B* **99**, 085120 (2019).

33. Y. Tokiwa, J. J. Ishikawa, S. Nakatsuji, P. Gegenwart, Quantum criticality in a metallic spin liquid. *Nat. Mater.* **13**, 356–359 (2014).

34. M. Kavai, J. Friedman, K. Sherman, M. Gong, I. Giannakis, S. Hajinazar, H. Hu, S. E. Grefe, J. Leshen, Q. Yang, S. Nakatsuji, A. N. Kolmogorov, Q. Si, M. Lawler, P. Aynajian, Inhomogeneous Kondo-lattice in geometrically frustrated Pr$_2$Ir$_2$O$_7$. *Nat. Commun.* **12**, 1377 (2021).

35. S. Nakatsuji, K. Kuga, Y. Machida, T. Tayama, T. Sakakibara, Y. Karaki, H. Ishimoto, S. Yonezawa, Y. Maeno, E. Pearson, G. G. Lonzarich, L. Balicas, H. Lee, Z. Fisk, Superconductivity and quantum criticality in the heavy-fermion system β-YbAlB$_4$. *Nat. Phys.* **4**, 603–607 (2008).

36. S. Paschen, H. Winkler, T. Nezu, M. Kriegisch, G. Hilscher, J. Custers, A. Prokofiev, Anisotropy of the Kondo insulator CeRu$_4$Sn$_6$. *J. Phys. Conf. Series* **200**, 012156 (2010).

37. G. Venturini, B. C. El Idrissi, J. F. Marêché, B. Malaman, Crystal structure and electrical properties of tetragonal YRu$_4$Sn$_6$. *Mater. Res. Bull.* **25**, 1541–1546 (1990).

38. I. Das, E. V. Sampathkumaran, Electrical-resistance anomalies in a Ce-Ru-Sn phase. *Phys. Rev. B* **46**, 4250–4252 (1992).

39. A. Prokofiev, S. Paschen, Crystal growth and stoichiometry of strongly correlated intermetallic cerium compounds, in *Modern Aspects of Bulk Crystal and Thin Film Preparation*, N. Kolesnikov, E. Borisenko, Eds. (InTech - Open Access Publisher, 2012), chap. 11, pp. 263–284.

40. G. Shirane, S. M. Shapiro, J. M. Tranquada, *Neutron Scattering with a Triple-Axis Spectrometer* (Cambridge Univ. Press, 2009).

41. G. Xu, J. F. Di Tusa, T. Ito, K. Oka, H. Takagi, C. Broholm, G. Aeppli, Y$_2$BaNiO$_5$: A nearly ideal realization of the $S = 1$ Heisenberg chain with antiferromagnetic interactions. *Phys. Rev. B Condens. Matter.* **54**, R6827–R6830 (1996).

Science Advances

Pristine quantum criticality in a Kondo semimetal

Wesley T. Fuhrman, Andrey Sidorenko, Jonathan Hänel, Hannes Winkler, Andrey Prokofiev, Jose A. Rodriguez-Rivera, Yiming Qiu, Peter Blaha, Qimiao Si, Collin L. Broholm and Silke Paschen

ARTICLE TOOLS	http://advances.sciencemag.org/content/7/21/eabf9134
SUPPLEMENTARY MATERIALS	http://advances.sciencemag.org/content/suppl/2021/05/17/7.21.eabf9134.DC1
REFERENCES	This article cites 39 articles, 7 of which you can access for free http://advances.sciencemag.org/content/7/21/eabf9134#BIBL
PERMISSIONS	http://www.sciencemag.org/help/reprints-and-permissions

Use of this article is subject to the Terms of Service